Research Article

iMedPub Journals
www.imedpub.com

Health Science Journal
ISSN 1791-809X

2022
Vol. 16 No. 3: 936

DOI: 10.36648/1791-809X.16.4.936

Differential Inhibitory Effects of Cytotoxic Agents on Lymphoma Cell Proliferation and Tumor Growth

Qiping Zheng[1,2]*, Lichun Sun[1,3]*Jinlei Ye[1], Mengli Yang[1], Shilei Wang[1], Ying Chen[1], Xiaojing Zhang[1,2], Chen Chen[2], Songhai Shen[1]

1 Shenzhen Academy of Peptide Targeting Technology at Pingshan and Shenzhen Tyercan Bio-Pharm Co, Ltd, Guangdong, 518118, China

2 Department of Haematological Laboratory Science, Jiangsu Key Laboratory of Medical Science and Laboratory Medicine, School of Medicine, Jiangsu University, Zhenjiang, 212013, China

3 Department of Medicine, School of Medicine, Tulane University Health Sciences Center, New Orleans, USA

***Corresponding author:**
Qiping Zheng

qp_zheng@hotmail.com, peptide612@gmail.com

Lichun Sun Shenzhen Academy of Peptide Targeting Technology at Pingshan and Shenzhen Tyercan Bio-Pharm Co Ltd, Guangdong, 518118, China

Citation: Zheng Q, Sun L, Ye J, Yang M, Wang S, et al. (2022) Differential Inhibitory Effects of Cytotoxic Agents on Lymphoma Cell Proliferation and Tumor Growth. Health Sci J. Vol. 16 No. 4: 936.

Abstract

In the last few decades, many biomolecules obtained from nature exhibit great potential in antitumor application, some of them have made great contributions to clinical treatment. Ansamitocin P3 and paclitaxel are tubulin inhibitors while camptothecin is a Topo I inhibitor. These molecules are known to induce apoptosis of cancer cells and either has been used or show great potential in application of tumor targeted therapy. In this study, we investigated the roles and mechanisms of ansamitocin P3, paclitaxel and camptothecin in inducing apoptosis of human histolytic lymphoma U937 cells. CCK8 assay was performed on U937 cells and the results showed that ansamitocin P3 exhibits great antiproliferative activities with a half-maximal inhibitory concentration (IC 50) at 0.18 ± 0.04 nM, while the IC50 of camptothecin and paclitaxel was 25.09 ± 2.64 and 6.06 ± 1.24 nM respectively. Results of apoptosis analysis by flow cytometry indicated that both early and late apoptotic cells increased significantly after treated with above three biomolecules. Cell cycle analysis results suggested that ansamitocin P3 and paclitaxel arrested cells in the G2/M Phase, while camptothecin arrested cells in G2/M phase at low concentration but S phase at high concentration. Mechanistically, we have performed expression analysis using qRT-PCR and found that ansamitocin P3 and paclitaxel may induce apoptosis of cells by down regulating expression of PCNA and BCL-2, while cells treated with camptothecin showed upregulated P21 but down regulated BCL-2 expression. Moreover, to investigate the in vivo anti-tumor activity of ansamitocin P3, we have shown data in a xenograft tumor model that ansamitocin P3 greatly inhibited tumor growth with little side effect. Taken together, our results suggest the strongest antitumor activity of ansamitocin P3 on lymphoma U937 cells. Ansamitocin P3 has great potential in tumor targeted therapy.

Keywords: Lymphoma cells; Ansamitocin P3; Paclitaxel; Camptothecin; Apoptosis; Tumor growth

Received: 04-Apr-2022, Manuscript No. Iphsj-22-12703; **Editor assigned:** 06-Apr-2022, PreQC No. Iphsj-22-12703 (PQ); **Reviewed:** 20-Apr-2022, QC No. Iphsj-22-12703, **Revised:** 25-Apr-2022, Manuscript No. Iphsj-22-12703(R); **Published:** 03-May-2022, DOI: 10.36648/1791-809X.16.3.936

Introduction

Lymphoma is a malignant tumor originating from the lymphatic hematopoietic system. Although it is more likely to occur in lymph nodes, it can invade almost any tissues and organs in the body due to flow of the lymphatic system, making the treatment effect unsatisfactory, especially in non-Hodgkin lymphoma **[1, 2].** In recent years, there has been extensive research on tumor targeted therapy. By targeting tumor cells, drugs are able to attack tumors accurately, achieve ideal efficacy with little damage to normal cells **[3].** As shown in the research of antibody-drug conjugate (ADC), as a key aspect of tumor targeted drugs, small molecules should have a suitable half maximal inhibitory concentration (IC_{50}) value **[4, 5],** so the selection of small molecules is critical and also challenging for drug development.

In the long history of antitumor research, a lot of active ingredients extracted from plants and microorganisms have exhibited strong antitumor activities **[6, 7].** The microtubules (MTs), which play an essential role in mitosis, have been commonly used as targets for cancer therapy **[8-10].** Ansamitocin P3 is an analogue of maytansine discovered in Nocardia species **[11].** It has been

known to disrupt the assembly of microtubules by binding to tubulin at the same site with vinblastine **[12].** After treatment with ansamitocin P3, cells were arrested in mitotic phase and apoptosis was induced. Although ansamitocin P3 shows great cytotoxicity, it has not been approved for clinical purpose due to its severe side effects and narrow therapeutic spectrum **[13].**

Paclitaxel, another molecule isolated from Pacific yew tree Taxus brevifolia, is one of the most widely used drug against many kinds of cancers **[14-16].** As a microtubule-stabilizing drug, it can make chromosomes non-segregation, cause mitotic arrest and induce apoptosis of cells **[17, 18].** Since first authorized in the treatment of ovarian and breast cancer by FDA, paclitaxel has been approved for treatment of many kinds of Tumors **[19, 20]**. However, the high toxicity and low solubility of paclitaxel make it imperfect as a drug candidate; so, nanotechnology was then established to improve the solubility and safety of paclitaxel **[21, 22].**

Camptothecin (CPT), which is a pentacyclic alkaloid extracted from Camptotheca acuminata, also exhibits good antitumor effect and has been used in tumor therapy for decades **[23-25].** It is a Topo inhibitor which can disrupt the replication of DNA and lead to apoptosis **[26].** Irinotecan, a camptothecin-derived drug, has been approved in the treatment of several advanced cancers since 1994 [27, 28]. However, the application of camptothecin was also limited due to its heavy toxicity and poor solubility **[24, 29].**

With the development of biomolecule conjugation technology and tumor targeting therapy, a lot of biomolecules show great potential to be developed as targeted antitumor drugs **[30].** In this study, we compared the antitumor effect of ansamitocin P3, paclitaxel and camptothecin on lymphoma U937 cells, investigated the potential mechanisms relating to apoptosis, and explored the inhibition effect of ansamitocin P3 in the xenograft tumor model, so as to identify appropriate therapeutic molecules suitable for targeting lymphoma or other cancer cells.

Materials and methods

Cell lines and cell culture

Human histolytic lymphoma U937 cells were purchased from Shanghai Cell Bank of the Chinese Academy of Sciences and cultured in RPMI-1640 medium supplied with 10% fetal bovine serum and 1% penicillin-streptomycin, and all of these reagents were supplied by Gibco (Thermo Fisher Scientific). Cells were incubated at 37°C and maintained in the condition of 5% CO_2.

Chemicals

Ansamitocin P3 (purity > 98%), paclitaxel (purity 99.97%) and camptothecin (purity 99.69%) were purchased from MCE (Med Chem Express, NJ, USA). PBS, RNase A was obtained from Solarbio (Solarbio Life Science, Beijing, China). Matrigel basement membrane matrix was supplied by BD Biosciences.

Cell Counting Kit-8 assay

The survival rate of cells after treated with biomolecules was assessed with Cell Counting Kit-8 colorimetric assay (Dojindo, Kumamoto, Japan). First, U937 cells were seeded into 96-well plates at 8×10^3 cells per well, then incubated with different concentrations of ansamitocin P3, paclitaxel and camptothecin (from 10^{-13} M to 10^{-6} M) for 72 hours. After adding 10 µl of Cell Counting Kit-8 solution into each of the wells for two hours, the OD values of the cells were recorded at 450 nm with the micro plate reader (Biotek, USA).

Cell cycle analysis

Cells were seeded into six-well plates for 2×10^5 cells per well, and treated with different concentrations of drugs for 24 hours. After collected and washed with PBS, cells were fixed with 70% ethanol at -20°C for several hours to days, then centrifuged at 4000 rpm for 2 minutes. Cell pellets were then resuspended in 500 µl PBS containing 0.25% Triton-X 100 and incubated on ice for 15 minutes. Then repeated centrifugation, and added 500 µl PBS with 10 µg/ml RNase A and 20 µg/ml PI to resuspend cells and incubated in the dark place at room temperature for 30 minutes. Finally, cell cycle was analysed using the flow cytometer (Beckman, USA). Data were analyzed with ModFit LT 5.0 (Trial version).

Apoptosis analysis

For apoptosis analysis, cells were seeded into six-well plates at 2×10^5 cells per well, and treated with ansamitocin P3, camptothecin and paclitaxel at different concentrations for 48 hours. After collected and washed with PBS, cells were suspended in 100 µl binding buffer and incubated with 5 µl FITC-AV and 5 µl PI (binding buffer, FITC-AV, PI were supplied within the detection kit) for 15 minutes. Finally, after 400 µl binding buffer was added, samples were detected on the flow cytometer. Data were analyzed with FlowJo V10 (Trial version).

mRNA expression analysis

Total RNA was extracted with Total RNA Kit (OMEGA, USA) and measured with Nano Drop micro volume spectrophotometer (Thermo Fisher Scientific, Waltham, MA, USA). Then reverse transcription was conducted with 1 µg RNA using the cDNA Synthesis kit (Genecopoeia, USA). Quantitative real-time PCR was performed by CFX Connect Real-Time System (Bio-Rad, USA) with 2 µl cDNA template and 2 µl primer according to the SYBR Green qPCR Mix 2.0 Kit (Genecopoeia, USA). *GAPDH* primers were purchased from Genecopoeia and other primers were supplied by Sangon Biotech. Primer sequences are each sample was tested triplicate in three tubes. The reaction procedure was set as follows: initial denaturation at 95°C for 30 seconds, then repeat 40 cycles at 95°C for 10 seconds to denature and 65°C for 30 seconds as annealing/extension, fluorescent intensity was detected at the end of every cycle. The data was analyzed with the comparative threshold cycle ($2^{-\Delta\Delta Ct}$) and taking *GAPDH* as control **(Table 1).**

Xenograft mouse tumor model

Five weeks-old female SCID mice were purchased from Beijing Vital River Laboratory Animal Technology Co., Ltd. in China and reared in SPF condition. Before the experiment, mice were raised for one week to adapt to the new environment. U937 cells (1

Table 1. Primer sequences of PCNA, P63, P21 and BCL-2.

	Primer sequence	
PCNA	Forward	TTAGCTCCAGCGGTGTAAAC
	Reverse	TTTGGACATACTGGTGAGGTTC
P63	Forward	CGTGTTATTGATGCTGTGCG
	Reverse	GAAGTCATTCCACTCATCTCGG
P21	Forward	TGTCACTGTCTTGTACCCTTG
	Reverse	GCGTTTGGAGTGGTAGAAATC
BCL-2	Forward	TTGTGGCCTTCTTTGAGTTCGGTG
	Reverse	GGTGCCGGTTCAGGTACTCAGTCA

× 10^6) were resuspended in PBS with Matrigel (ratio 1:1, total volume 100 µl) and injected subcutaneously into the right flank of each mouse. Tumor volumes were calculated as 0.5 × Length × Width^2, When the tumor size reached 70-120 mm^3, mice were divided into the control group and the treatment/experimental (ansamitocin P3) group. Mice in the experimental group received ansamitocin P3 (0.4 mg/kg, 100 µl) by tail vein injection while mice in the control group were given 100 µl normal saline containing 10% alcohol. Mice were treated every two weeks for four weeks. Tumor measurements and bodyweights were recorded twice a week. The protocol was approved by Shanghai Medicilon IACUC (approval number: TEK2103P).

Statistical analysis

IC_{50} values were acquired and analyzed by Graph Pad 8.3.0. All experiments were done at least three times and mean ± SD was calculated. Statistical significance was determined by t-test, $p < 0.05$ was recognized as significant.

Results

Differential cytotoxic activity of ansamitocin P3, camptothecin, and paclitaxel on U937 cells

To compare their cytotoxicity, we measured the cell viability of U937 cells using the CCK8 assay kit after cells were treated with above three compounds for 72 hours. The results indicated that treatment with these drugs can significantly and differentially inhibit U937 cell proliferation. ansamitocin P3, camptothecin and paclitaxel all inhibited the cell viability of U937 in a dose-dependent manner. When increased the concentration of the compounds, the viability of U937 cells rapidly decreased to extremely low level. With the concentration of ansamitocin P3, camptothecin, and paclitaxel at 1 nM, 50 nM and 10 nM, the cell viabilities of U937 cells reduced to about 2%, 7%, and 5% respectively. In all groups, the cell viability reduced to about 2% when the compounds were at highest concentration. Half-maximal proliferation inhibitory concentrations (IC_{50}) of ansamitocin P3, camptothecin, and paclitaxel in U937 cells were at about 0.18 ± 0.04, 25.09 ± 2.64 and 6.06 ± 1.24 nM respectively, suggesting that these compounds have strong antitumor activities with ansamitocin P3 showed the strongest antitumor effect **(Figure 1).**

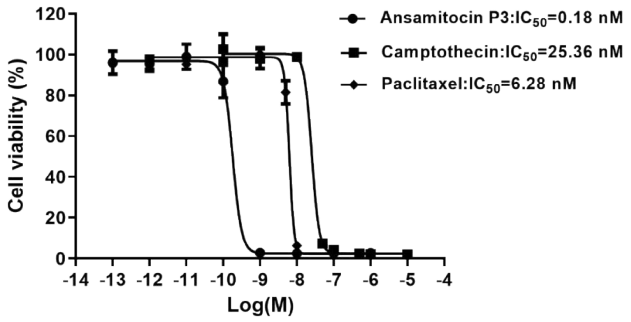

Figure 1 Cell viability of U937 cells after treated with ansamitocin P3, camptothecin and paclitaxel for 72 hours. The concentrations of ansamitocin P3 were set from 10^{-13} M to 10^{-6} M. The concentrations of camptothecin were set from 10^{-10} M to 10^{-5} M with $5*10^{-8}$ M and $5*10^{-7}$ M. The concentrations of paclitaxel were set from 10^{-12} M to 10^{-6} M with $5*10^{-9}$ M. The IC_{50} values of ansamitocin P3, camptothecin and paclitaxel in U937 cells were at about 0.2, 25, 6 nM respectively.

Cells were arrested in G2/M or S phase after treatment with above compounds

In order to evaluate their effect on cell cycle, cells were treated with the above three compounds in three concentrations near IC_{50} for 24 hours and analyzed by flow cytometry. it is obvious that after treated with ansamitocin P3 and paclitaxel, large amounts of cells accumulated in G2/M phase. However, in the camptothecin group, it showed different effect in two concentrations, most cells were arrested in G2/M phase at 25 nM but in S phase at 50 nM **(Figure 2).**

Percentages of cells in different cell cycle phase When the concentration of ansamitocin P3 and paclitaxel increased from 0.1 nM to 0.4 nM and from 3 nM to12 nM respectively, percentage of cells in G2/M phase increased from about 30% to more than 60% while cells in G0/G1 and S phase were reduced. For camptothecin ranged from 12.5 nM to 25 nM, percentage of cells in G0/G1 phase reduced from about 30% to 15%, and percentage of cells in G2/M phase increased from about 45% to 60%. However, when the concentration of camptothecin reached 50 nM, percentage of cells in S phase increased to about 60% while cells in G2/M phase reduced to about 30% **(Table 2).**

U937 cell apoptosis induced by ansamitocin P3, camptothecin and paclitaxel

After treated with the above three compounds for 48 hours, percentage of apoptotic U937 cells was detected by flow cytometry. As shown in **(Figure 3),** the percentages of early (Q3) and late (Q2) apoptotic cells both increased obviously in the treated group, indicating the great pro-apoptotic effect of these compounds on U937 cells.

The percentages of apoptotic cells of U937 after treated with different concentrations of the three compounds were. In the control group, the total percentage of the apoptotic cells

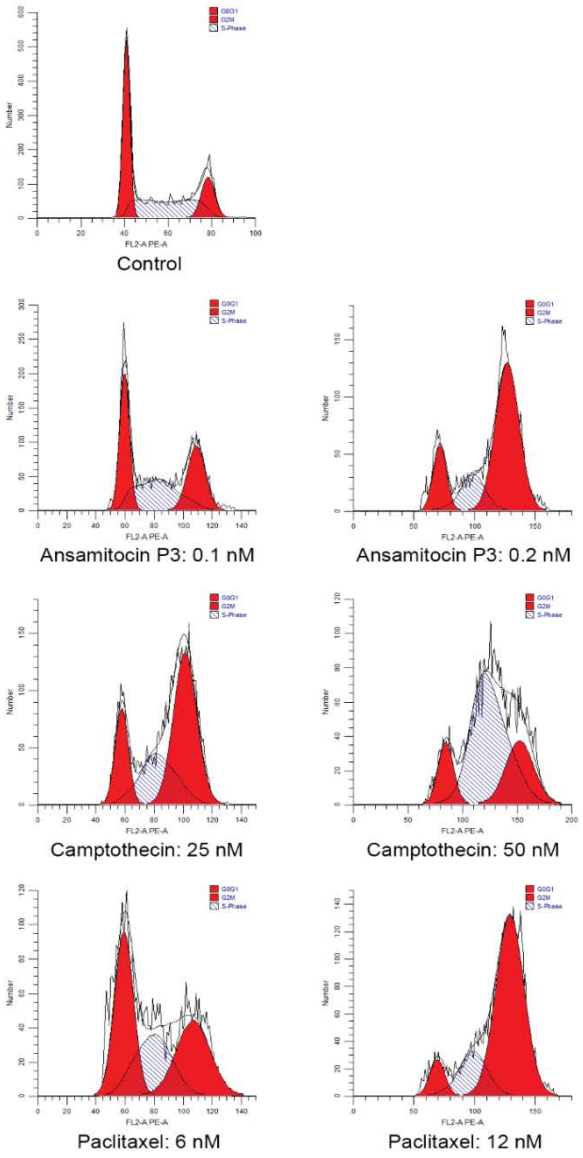

Figure 2 Cell cycle changes arrested by ansamitocin P3, camptothecin and paclitaxel. Data were analyzed by ModFit, G0G1, G2M and S-Phase represent cells in G0/G1, G2/M and S phase respectively. The concentrations of ansamitocin P3, camptothecin and paclitaxel were at 0.1/ 0.2, 25/50 and 6/12 nM respectively. After treatment with high concentration of compounds for 24 hours, a great amount of U937 cells was arrested in G2/M phase in ansamitocin P3 and paclitaxel treated group but S phase in camptothecin treated group.

was about 4.43 ± 0.25%. In ansamitocin P3 treated group with the concentration of drug ranged from 0.1 nM to 0.4 nM, the percentage of apoptotic cells increased from 24.83 ± 0.13% to 83.31 ± 0.47%. Meanwhile, for camptothecin and paclitaxel ranged from 12.5 nM to 50 nM, and from 3 nM to 12 nM, the percentage of apoptotic cells increased from 5.54 ± 1.78% to 54.65 ± 2.62% and from 7.17 ± 0.20% to 82.23 ± 4.77% respectively. These results demonstrated that all three compounds were able

Table 2. Percentages of cells in different phases of cell cycle after treatment with compounds for 24 hours.

	Concentration (nM)	G0/G1 phase (%)	S phase (%)	G2/M phase (%)
Control		44.82 ± 2.16	36.67 ± 2.33	18.52 ± 0.17
Ansamitocin P3	0.1	36.10 ± 1.53	34.06 ± 1.21	29.84 ± 0.33
	0.2	16.03 ± 0.66	15.58 ± 2.21	68.40 ± 2.86
	0.4	6.02 ± 2.91	18.62 ± 2.62	75.37 ± 5.53
Camptothecin	12.5	30.16 ± 3.34	35.60 ± 1.43	34.24 ± 1.91
	25	16.95 ± 3.22	27.83 ± 0.48	55.23 ± 2.74
	50	10.65 ± 3.42	70.82 ± 11.24	18.54 ± 7.81
Paclitaxel	3	40.56 ± 2.90	33.32 ± 8.81	26.12 ± 5.92
	6	32.70 ± 9.02	33.70 ± 7.09	33.61 ± 1.93
	12	5.59 ± 1.80	27.01 ± 12.30	66.41 ± 10.50

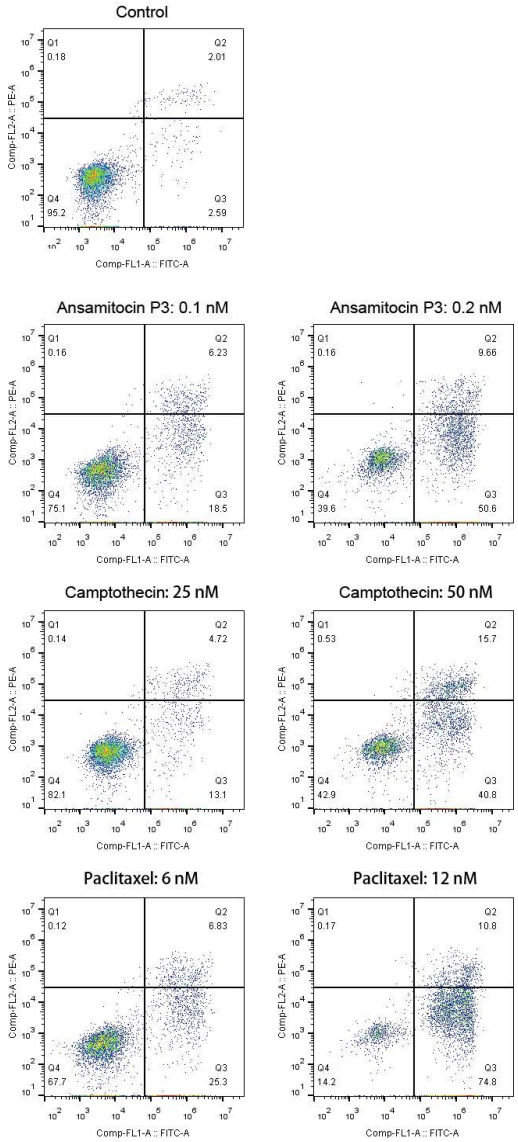

Figure 3 Cell apoptosis in histiocytic lymphoma U937 cells induced by ansamitocin P3, camptothecin and paclitaxel. Q1, Q2, Q3, Q4 represent dead, late apoptotic, early apoptotic and live cells respectively. The concentration settings of above compounds were the same as cell cycle analysis. After treated with the three compounds, both early and late apoptotic cells increased obviously.

to induce cell apoptosis and that increase of apoptotic cells was positively correlated with drug concentration (**Table 3)**.

Altered expression of BCL-2, P21 and PCNA in cells treated with ansamitocin P3, camptothecin and paclitaxel

To study the putative mechanism of cell apoptosis induced by the three compounds, U937 cells were treated for 24 hours with 0.2 nM ansamitocin P3, 50 nM camptothecin, and 12 nM paclitaxel respectively. Then, the mRNA levels of *BCL-2*, *P21*, *P63* and *PCNA* (proliferating cell nuclear antigen) were analyzed by qPCR. As shown in (**Figure 4)**, *BCL-2* was down regulated in all the cells treated with either of the three compounds, which is consistent with the results of high percentages of apoptotic cells. Besides, decreased expression of *PCNA* mRNA was detected in ansamitocin P3 and paclitaxel groups ($P < 0.05$), but no significant difference was observed in camptothecin treated group compared with the control group.

Table 3. Percentages of apoptotic cells in U937 after treated with the compounds.

	Concentration (nM)	Early apoptotic cells (%)	Late apoptotic cells (%)	Total Apoptotic cells (%)
Control		2.55 ± 0.06	1.88 ± 0.19	4.43 ± 0.25
Ansamitocin P3	0.1	18.55 ± 0.07	6.28 ± 0.06	24.83 ± 0.13
	0.2	54.90 ± 6.08	10.23 ± 0.81	65.13 ± 6.89
	0.4	74.10 ± 0.85	9.21 ± 0.38	83.31 ± 0.47
Camptothecin	12.5	3.43 ± 1.13	2.11 ± 0.65	5.54 ± 1.78
	25	12.10 ± 1.41	5.04 ± 0.45	17.14 ± 0.97
	50	37.80 ± 4.24	16.85 ± 1.63	54.65 ± 2.62
Paclitaxel	3	4.80 ± 0.64	2.38 ± 0.45	7.17 ± 0.20
	6	27.35 ± 2.90	7.51 ± 0.96	34.86 ± 3.85
	12	73.10 ± 2.40	9.13 ± 2.37	82.23 ± 4.77

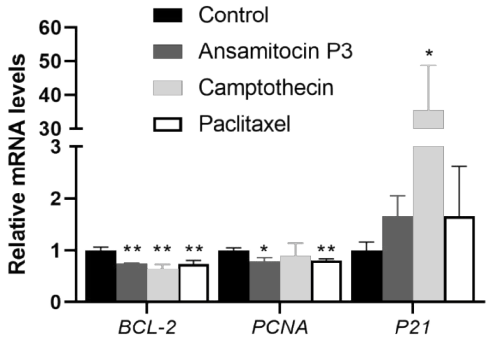

Figure 4 Relative mRNA levels of *BCL-2*, *P21* and *PCNA* in U937 cells. U937 cells were subjected to 24 hours exposure to 0.2 nM ansamitocin P3, 50 nM camptothecin and 12 nM paclitaxel respectively. *BCL-2* expression was down regulated in three groups. *PCNA* expression was down regulated in ansamitocin P3 and paclitaxel groups. *P21* expression was down regulated in camptothecin group. Statistical significance was determined by t-test (* represents $p < 0.05$ and ** represents $p < 0.01$).

To understand the effect of cell cycle arrest, we examined the expression of *P21*. After treated with camptothecin, *P21* expression was obviously upregulated. However, for ansamitocin P3 and paclitaxel group, *P21* mRNA was slightly upregulated without significant difference compared with that of the control groups.

In addition, we examined *P63* expression in the cells, and it was barely detectable in all the cells with or without treatment with the three compounds (data not shown).

Ansamitocin P3 inhibited tumor growth of U937 in vivo

To further investigate the antitumor efficacy of ansamitocin P3, U937 xenograft mouse tumor models were established. When the tumors reached size at 70-120 mm^3, the mice were separated into two groups (n=8 each): the control (PBS) group and ansamitocin P3 treated group, which was administered by tail vein injection at the concentration of 0.4 mg/kg for 100 µl. and **(Table 4)**, in the control group, tumor volumes increased from 94.96 ± 12.03 mm^3 (Day 0) to 3530.20 ± 1595.66 mm^3 (Day 17). According to the requirement of the ethics of animal experiments, the mice in the control group were sacrificed at day 17. In ansamitocin P3 treated group, tumor volumes of mice rose from 95.28 ± 9.98 mm^3 (Day 0) to 2749.61 ± 1442.53 mm^3 (Day 24). When giving ansamitocin P3 at a low dose of 0.4 mg/kg every two weeks, the relative tumor proliferation rate (T/C, %) was 29.98 at day 17, while bodyweights slightly decrease after treated **(Figure 5 and Table 5).** The detailed information of each mouse analyzed was shown in (**Table 6)**. The results support that ansamitocin P3 inhibited tumor growth of the U937 xenograft tumor model.

Discussion and Conclusion

Ansamitocin P3, paclitaxel and camptothecin are antitumor biomolecules with great effects. In this study, we first compared the cytotoxic effect of ansamitocin P3, paclitaxel and camptothecin on U937 lymphoma cells in vitro. No more than 10% cells survived after treatment with these three compounds, and ansamitocin P3 showed the strongest anti-tumor effect with lowest IC_{50}.

In cell cycle analysis, a lot of cells were arrested in G2/M phase when cells were treated with increased concentration of ansamitocin P3 and paclitaxel. As tubulin inhibitors, ansamitocin P3 and paclitaxel have previously been shown to arrest U937 cells in mitosis **[8, 12].** In our study, cells were arrested in G2/M phase when treated with low concentration of camptothecin but S phase at high concentration, which may be related to Topo I activity as previously reported **[31].** Low concentration of camptothecin might cause low levels of DNA damage, and thus, the cells accumulate at G2 check point **[32].** When treated with high concentration of camptothecin, cells might suffer severe DNA damage and thus arrested in S phase.

Apoptosis analysis results showed that after treatment with three compounds for 48 hours, percentages of early and late apoptotic cells were all increased, which was positively correlated with drug concentration. High concentration of compounds induced

Table 4. Comparation of tumor volumes between control group and treated group.

Days Post Treatment			0	3	7	10	14	17	21	24
Control group	Tumor Volume (mm^3)	Mean	94.96	145.94	302.14	682.34	1579.61	3530.2	/	/
		SD	12.03	45.23	147.91	252.95	725.9	1595.66	/	/
		SEM	4.55	17.09	55.9	95.61	274.36	603.1	/	/
	Relative Tumor Volume	Mean	1	1.55	3.18	7.16	16.62	36.92	/	/
		SD	0	0.5	1.62	2.57	7.89	16.4	/	/
		SEM	0	0.19	0.61	0.97	2.98	6.2	/	/
Ansamitocin P3 group	Tumor Volume (mm^3)	Mean	95.28	117.1	156.71	353.92	843.29	1088.91	1431.42	2749.61
		SD	9.98	13.6	38.91	199.16	556.15	710.3	893.1	1442.53
		SEM	3.77	5.14	14.71	75.28	210.2	268.47	337.56	545.23
	Relative Tumor Volume	Mean	1	1.23	1.64	3.64	8.55	11.07	14.62	28.28
		SD	0	0.14	0.33	1.88	5.21	6.67	8.56	14.16
		SEM	0	0.05	0.13	0.71	1.97	2.52	3.23	5.35
	% T/C		100	79.35	51.57	50.84	51.44	29.98	/	/

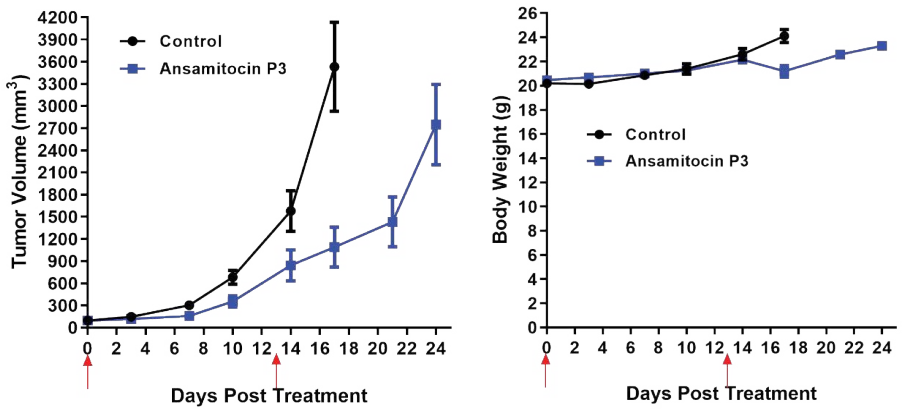

Figure 5 Ansamitocin P3 exhibited suppressive effect on U937 tumor growth in nude mice. Ansamitocin P3 (0.4 mg/kg, 100 µl) was administrated by tail vein injection every two weeks for four weeks, while normal saline containing 10% alcohol were injected in the control group. At day 0, tumor volumes were 94.96 ± 12.03 mm^3 in control group and 95.28 ± 9.98 mm^3 in ansamitocin P3 group, with 3530.20 ± 1595.66 mm^3 in control group at day 17 and 2749.61 ± 1442.53 mm^3 in ansamitocin P3 group at day 24 (left panel). Compared with mice in control group, bodyweights of mice in ansamitocin P3 group slightly decreased after treated (right panel). Data in the graph are presented as the mean ± S.E.M.

Table 5. Body weights and changes in control group and ansamitocin P3 group.

Days Post Treatment			0	3	7	10	14	17	21	24
Control group	Body Weight (g)	Mean	20.19	20.14	20.87	21.39	22.59	24.11	/	/
		SD	0.89	0.87	0.87	1.14	1.29	1.46	/	/
		SEM	0.34	0.33	0.33	0.43	0.49	0.55	/	/
	Change (g)		0	-0.05	0.68	1.2	2.4	3.92	/	/
Ansamitocin P3 group	Body Weight (g)	Mean	20.47	20.68	21	21.25	22.15	21.19	22.58	23.3
		SD	0.49	0.72	0.83	0.91	0.66	1.26	0.76	0.89
		SEM	0.19	0.27	0.32	0.35	0.25	0.48	0.29	0.34
	Change(g)		0	0.21	0.53	0.78	1.68	0.72	2.11	2.83

more than half of the cells to undergo apoptosis, suggesting the great antitumor effect.

To further explore the difference of mechanisms by which the compounds exhibit their inhibition effects, expressions of several genes were analyzed by qPCR. BCL-2 was known as a typical anti-apoptotic protein **[33-35]**, and was down regulated in all the cells treated with either of the three compounds. Proliferating cell nuclear antigen (PCNA), which was known to function in DNA replication and repair, is also involved in apoptosis

Table 6. Tumor sizes and body weights of mice in two group.

	Animal #			Days Post Treatment							
				0	3	7	10	14	17	21	24
Control Group	1	Tumor Size	Length (mm)	6.36	7.05	10.16	13.88	16.92	21.95	/	/
			Width (mm)	5.98	6.45	8.9	11.58	15.38	20.45	/	/
		Body Weight (g)		21.88	21.42	22.39	23.5	24.02	24.75	/	/
	2	Tumor Size	Length (mm)	6.01	7.15	10.92	14.74	16.86	23.72	/	/
			Width (mm)	5.84	5.91	6.7	9.74	13.18	19.41	/	/
		Body Weight (g)		19.61	19.55	20.14	21.06	22.73	24.51	/	/
	3	Tumor Size	Length (mm)	6.24	7.8	9.88	11.56	15.04	19.43	/	/
			Width (mm)	5.58	5.68	6.6	9.91	14.48	19.34	/	/
		Body Weight (g)		20.68	20.09	20.83	21.26	22.68	24.21	/	/
	4	Tumor Size	Length (mm)	6.24	8.31	9.5	12.09	13.7	17.05	/	/
			Width (mm)	5.55	7.11	7.4	9.53	11.48	14.3	/	/
		Body Weight (g)		20.38	21.22	21.4	21.26	21.85	23.52	/	/
	5	Tumor Size	Length (mm)	5.88	6.25	9.08	11.08	14.31	18.95	/	/
			Width (mm)	5.59	5.71	7.41	9.68	13.89	15.97	/	/
		Body Weight (g)		20.04	20.11	20.84	20.82	22.03	23.09	/	/
	6	Tumor Size	Length (mm)	5.81	8.9	13.87	15.06	20.59	29.49	/	/
			Width (mm)	5.52	6.82	9.23	12.15	16.9	20.16	/	/
		Body Weight (g)		19.42	19.32	20.8	22.02	24.3	26.64	/	/
	7	Tumor Size	Length (mm)	5.56	6.67	8.48	12.14	13.8	19.58	/	/
			Width (mm)	5.19	5.62	5.99	8.11	10.71	13.81	/	/
		Body Weight (g)		19.35	19.28	19.69	19.81	20.54	22.02	/	/
Ansamitocin P3 Group	8	Tumor Size	Length (mm)	6.53	6.79	6.84	8.87	12.96	13.96	15.43	20.01
			Width (mm)	5.84	6.11	6.3	8.64	12.88	13.31	14.45	18.49
		Body Weight (g)		19.55	19.39	19.51	19.44	21.21	18.73	21.38	22.09
	9	Tumor Size	Length (mm)	6.63	6.7	10.4	15.9	19.84	19.99	20.2	24.27
			Width (mm)	5.62	6.15	6.53	9.12	13.43	15.36	16.68	18.57
		Body Weight (g)		20.21	20.16	20.24	20.88	21.96	21.3	22.44	23.43
	10	Tumor Size	Length (mm)	6.1	6.31	7.47	12.42	16.81	16.9	18.2	22.04
			Width (mm)	5.64	5.84	7.28	9.62	11.32	12.9	15.04	18.65
		Body Weight (g)		20.24	20.54	21.8	22.16	22.63	22.68	23.75	24.84
	11	Tumor Size	Length (mm)	6.13	6.41	6.97	7.76	9.3	10.33	9.72	13.04
			Width (mm)	5.49	5.72	6.48	6.55	8.08	9.64	8.58	10.17
		Body Weight (g)		20.88	21.44	21.58	21.71	22.31	20.58	21.93	22.75
	12	Tumor Size	Length (mm)	6.03	6.7	7.2	11.64	16.96	17.01	17.03	21.25
			Width (mm)	5.5	6.44	6.47	7.01	8.55	9.57	11.73	16.9
		Body Weight (g)		20.82	21.36	21.58	21.62	22.91	21.45	22.8	23.62
	13	Tumor Size	Length (mm)	5.95	6.4	7.57	10.88	15.5	15.89	15.93	20.63
			Width (mm)	5.44	5.88	5.91	7.87	10.82	12.18	14.47	18.05
		Body Weight (g)		20.83	21.02	21.26	21.87	22.66	21.95	22.88	23.69
	14	Tumor Size	Length (mm)	5.9	6.99	7.06	7.45	7.55	8.1	9.62	12.47
			Width (mm)	5.28	5.46	5.64	5.7	5.89	6.74	8.45	10.89
		Body Weight (g)		20.74	20.86	21.02	21.06	21.4	21.67	22.9	22.7

signaling pathway **[36].** In previous study, *PCNA* was reported to be inhibited by paclitaxel in MG-63 cells **[37].** In this study, *PCNA* was down regulated after treatment with ansamitocin P3 and paclitaxel, suggesting their role of proliferation inhibition. However, no difference was observed between camptothecin-treated and the control group. P21 is a known cyclin-dependent kinase (CDK) inhibitor and apoptosis inhibitor **[38, 39].** Compared to the control groups, *P21* was obviously upregulated in camptothecin group as previously reported **[40],** while slightly increased in ansamitocin P3 and paclitaxel treated groups but without statistically significant difference. These results indicated that while differ from camptothecin, ansamitocin P3 and paclitaxel induced cell apoptosis via the same signaling pathway.

In the xenograft animal model, tumor volumes of mice under treatment of ansamitocin P3 were obviously smaller than the control group. At day 17, the relative tumor proliferation rate (T/C, %) was about 30, indicating the great antitumor effect of ansamitocin P3. Meanwhile, treatment for every two weeks only resulted a slight decrease for the bodyweight, suggesting insignificant side effect.

To summarize, we compared the effect of ansamitocin P3, paclitaxel and camptothecin in inhibition of U937 lymphoma cells in vitro and confirmed that ansamitocin P3 has the same mechanism in inducing apoptosis with paclitaxel and with stronger antitumor activity. The in vivo anti-tumor assay also showed that ansamitocin P3 inhibited tumor growth obviously with slight side effect. With the development of biomolecule conjugation technology and tumor targeting therapy, the biomolecules with high cytotoxicity are able to selectively kill tumor cells while reduce the side effect. Our results suggest that ansamitocin P3 shows great potential in the treatment of lymphoma and thus a suitable candidate biomolecule for tumor targeting therapy.

References

1 Armitage JO, Gascoyne RD, Lunning MA, Cavalli F (2017) Non-hodgkin lymphoma. Lancet 390: 298-310.

2 Freedman AS, LaCasce AS (2016) Non-H odgkin's Lymphoma. Hollan Cancer Med 1-19.

3 Wang L, Qin W, Huo Y-J, Li X, Shi Q (2020) Advances in targeted therapy for malignant lymphoma. Signal Transduct Tar 5:1-46.

4 Khongorzul P, Ling CJ, Khan FU, Ihsan AU, Zhang J (2020) Antibody–drug conjugates: a comprehensive review. Mol Cancer Res 18: 3-19.

5 Yaghoubi S, Karimi MH, Lotfinia M, Gharibi T, Mahi-Birjand M (2020) Potential drugs used in the antibody-drug conjugate (ADC) architecture for cancer therapy. J Cell Physiol 235:31-64.

6 Gezici S, Şekeroğlu N (2019) Current perspectives in the application of medicinal plants against cancer: novel therapeutic agents. Anti-Cancer Agent Me 19:101-111.

7 Chen L, Zhang Q-Y, Jia M, Ming Q-L, Yue W (2016) Endophytic fungi with antitumor activities: Their occurrence and anticancer compounds. Crit Rev Microbiol 42:454-473.

8 Steinmetz MO, Prota AE (2018) Microtubule-targeting agents: strategies to hijack the cytoskeleton. Trends Cell Biol 28:776-792.

9 Mukhtar E, Adhami VM, Mukhtar H (2014) Targeting microtubules by natural agents for cancer therapy. Mol Cancer Ther 13:275-284.

10 Lemjabbar-Alaoui H, Peto CJ, Yang Y-W, Jablons DM (2020) AMXI-5001 a novel dual parp1/2 and microtubule polymerization inhibitor for the treatment of human cancers. Am J Cancer Res 10: 2649.

11 Higashide E, Asai M, Ootsu K, Tanida S, Kozai Y (1977) Ansamitocin, a group of novel maytansinoid antibiotics with antitumour properties from Nocardia. Nature 270:721-722.

12 Venghateri JB, Gupta TK, Verma PJ, Kunwar A, Panda D (2013) Ansamitocin P3 depolymerizes microtubules and induces apoptosis by binding to tubulin at the vinblastine site. PloS one 8: e75182.

13 Cassady JM, Chan KK, Floss HG, Leistner E (2004) Recent developments in the maytansinoid antitumor agents. Chem Pharm Bull 52:1-26.

14 McGuire WP, Rowinsky EK, Rosenshein NB, Grumbine FC, Ettinger DS (1989) Armstrong DK and Donehower RC. Taxol: a unique antineoplastic agent with significant activity in advanced ovarian epithelial neoplasms. Ann Intern Med 111:273-279.

15 Marupudi NI, Han JE, Li KW, Renard VM, Tyler BM (2007) Paclitaxel a review of adverse toxicities and novel delivery strategies. Expert Opin Drug Saf 6:609-621.

16 Markman M, Mekhail TM (2002) Paclitaxel in cancer therapy. Expert Opin Pharmaco 3:755-766.

17 Wang TH, Wang HS, Soong YK (2000) Paclitaxel-induced cell death: where the cell cycle and apoptosis come together. Cancer: Interdisciplinary Inte Am J Canc Society 88:2619-2628.

18 Brito DA, Yang Z, Rieder CL (2008) Microtubules do not promote mitotic slippage when the spindle assembly checkpoint cannot be satisfied. J Cell Biol 182:623-629.

19 Alves RC, Fernandes RP, Eloy JO, Salgado HRN, Chorilli M (2018) Characteristics, properties and analytical methods of paclitaxel: a review. Crit Rev Anal Chem 48:110-118.

20 Alqahtani FY, Aleanizy FS, El Tahir E, Alkahtani HM, AlQuadeib BT (2019) Paclitaxel In: editors. Profiles of drug substances, excipients and related methodology. Elsevier 205-238.

21 Bernabeu E, Cagel M, Lagomarsino E, Moretton M, Chiappetta DA (2017) Paclitaxel: what has been done and the challenges remain ahead. Int J Pharmaceut 526:474-495.

22 Adrianzen Herrera D, Ashai N, Perez-Soler R, Cheng H (2019) Nanoparticle albumin bound-paclitaxel for treatment of advanced non-small cell lung cancer: an evaluation of the clinical evidence. Expert Opin Pharmaco 20: 95-102.

23 Martino E, Della Volpe S, Terribile E, Benetti E, Sakaj M et al. (2017) The long story of camptothecin: From traditional medicine to drugs. Bioorg Med Chem Lett 27:701-707.

24 Venditto VJ and Simanek EE (2010) Cancer therapies utilizing the camptothecins: a review of the in vivo literature. Mol Pharmaceut 7:307-349.

25 Li F, Jiang T, Li Q, Ling X (2017) Camptothecin (CPT) and its derivatives are known to target topoisomerase I (Top1) as their mechanism of action: did we miss something in CPT analogue molecular targets for treating human disease such as cancer? Am J Cancer Res 7:2350.

26 Liu LF, Desai SD, LI TK, Mao Y, Sun M (2000) Mechanism of action of camptothecin. Ann Ny Acad Sci 922:1-10.

27 Bailly C (2019) Irinotecan 25 years of cancer treatment. Pharmacol Res 148:104398.

28 Kciuk M, Marciniak B, Kontek R (2020) Irinotecan Still an important player in cancer chemotherapy: A comprehensive overview. Int J Mol Sci 21:4919.

29 Moertel CG, Schutt AJ, Reitemeier R, Hahn R (1972) Phase IT study of camptothecin (NSC-1 00880) in the treatment of advanced gastrointestinal cancer. Cancer Chemother Rep 56:95-101.

30 García-Alonso S, Ocaña A, Pandiella A (2020) Trastuzumab emtansine: mechanisms of action and resistance, clinical progress, and beyond. Trends Cancer 6:130-146.

31 Jones CB, Clements MK, Wasi S, Daoud SS (1997) Sensitivity to camptothecin of human breast carcinoma and normal endothelial cells. Cancer Chemoth Pharm 40:475-483.

32 Goldwasser F, Shimizu T, Jackman J, Hoki Y et al. (1996) Correlations between S and G2 arrest and the cytotoxicity of camptothecin in human colon carcinoma cells. Cancer Res 56:4430-4437.

33 Singh R, Letai A, Sarosiek K (2019) Regulation of apoptosis in health

and disease: the balancing act of BCL-2 family proteins. Nat Rev Mol Cell Bio 20:175-193.

34 Ashkenazi A, Fairbrother WJ, Leverson JD, Souers AJ (2017) From basic apoptosis discoveries to advanced selective BCL-2 family inhibitors. Nat Rev Drug Discov 16: 273-284.

35 Marquez RT, Xu L (2012) Bcl-2: Beclin complex: multiple, mechanisms regulating autophagy/apoptosis toggle switch. Am J Cancer Res 2:214.

36 González-Magaña A, Blanco FJ (2020) Human PCNA structure, function and interactions. Biomolecules 10:570.

37 Liu S-Y, Song S-X, Lin L, Liu X (2010) Molecular mechanism of cell apoptosis by paclitaxel and pirarubicin in a human osteosarcoma cell line. Chemotherapy 56:101-107.

38 Shamloo B, Usluer S (2019) in cancer research. Cancers 11:1178.

39 Karimian A, Ahmadi Y, Yousefi B (2016) Multiple functions of p21 in cell cycle, apoptosis and transcriptional regulation after DNA damage. DNA repair 42:63-71.

40 Chiu C-F, Lin Y-Q, Park JM, Chen Y-C, Hung S-W (2020) The novel camptothecin derivative, CPT211, induces cell cycle arrest and apoptosis in models of human breast cancer. Biomed Pharmacother 128:110309.